



Visual servoing with respect to complex objects

Andrew Comport, O. Tahri, E. Marchand, François Chaumette

► **To cite this version:**

Andrew Comport, O. Tahri, E. Marchand, François Chaumette. Visual servoing with respect to complex objects. Int. Symp. on Robotics, ISR'04, 2004, Paris, France, France. 2004. <inria-00352022>

HAL Id: inria-00352022

<https://hal.inria.fr/inria-00352022>

Submitted on 12 Jan 2009

HAL is a multi-disciplinary open access archive for the deposit and dissemination of scientific research documents, whether they are published or not. The documents may come from teaching and research institutions in France or abroad, or from public or private research centers.

L'archive ouverte pluridisciplinaire **HAL**, est destinée au dépôt et à la diffusion de documents scientifiques de niveau recherche, publiés ou non, émanant des établissements d'enseignement et de recherche français ou étrangers, des laboratoires publics ou privés.

Visual servoing with respect to complex objects

Andrew I. Comport, Omar Tahri, Éric Marchand, François Chaumette
IRISA / INRIA Rennes
Campus de Beaulieu, 35 042 Rennes-cedex, France
E-Mail : `Firstname.Lastname@irisa.fr`

Abstract

This paper presents new advances in the field of visual servoing. More precisely, we consider the case where complex objects are observed by a camera. In a first part, planar objects of unknown shape are considered using image moments as input of the image-based control law. In the second part, a pose estimation and tracking algorithm is described to deal with real objects whose 3D model is known. For each case, experimental results obtained with an eye-in-hand system are presented.

1 Introduction

Visual servoing has been widely studied in the past [6, 7]. In few words, it consists in controlling the velocity \mathbf{v} of a camera mounted on the end-effector of a robot to iteratively minimize the error $\mathbf{s} - \mathbf{s}^*$ between the current value (\mathbf{s}) and the desired one (\mathbf{s}^*) of a set of visual features computed from the data provided by the camera. The case where one or several cameras are simultaneously observing the scene and the robot end-effector can also be considered. A typical closed loop control law has the following form:

$$\mathbf{v} = -\lambda \widehat{\mathbf{L}}_{\mathbf{s}}^+ (\mathbf{s} - \mathbf{s}^*) \quad (1)$$

where λ is a proportional gain that has to be tuned to minimize the time-to-convergence, and where $\widehat{\mathbf{L}}_{\mathbf{s}}^+$ is the pseudo-inverse of a model or an approximation of the interaction matrix related to the visual features \mathbf{s} . This matrix plays an essential role in the behavior of the system. It is defined by the relation $\dot{\mathbf{s}} = \mathbf{L}_{\mathbf{s}} \mathbf{v}$.

In this paper, we present new results in visual servoing for positioning tasks with respect to complex objects. In the next section, planar objects of unknown shape are considered using an adequate set of image moments as visual features \mathbf{s} . In Section 3, a pose estimation and tracking algorithm is described to deal with real objects whose 3D model is known. In that case, any visual servoing scheme can be used: image-based (2D), position-based (3D), or hybrid scheme (2 1/2D). Experimental results obtained with an eye-in-hand system are presented in these two sections.

2 Visual servoing from image moments

2.1 Overview of the approach

In 2D visual servoing, the control of the robot motion is performed using data extracted directly from the images acquired by the camera. Several kinds of visual features have been proposed in the past. Most works have been concerned with known and simple objects. They assume that the objects in the scene can be expressed with simple features such as points, straight lines, or ellipses [6]. The group of the objects that these methods can be applied to is thus limited. The first interest of using image moments in visual servoing is that they provide a generic and geometrically intuitive representation of any object, with simple or complex shapes that can be segmented in an image. They can also be extracted from a set of image points tracked along an image sequence by simple summation of polynomials that depend on the points position.

Furthermore, an important problem in the visual servoing field is to determine the visual features to use in the control scheme in order to obtain an optimal behavior of the system. A necessary condition is first to ensure the convergence of the control loop. A good way to ensure this condition is to design a decoupled control scheme, i.e. to try to associate each camera degrees of freedom with only one visual feature. Such control would make easy the determination of the potential singularities of the considered task. A such totally decoupled control would be ideal but seems impossible to reach. It is however possible to decouple the translational motions from the rotational ones. This decoupled control can be obtained using moment invariants as fully described in [12]. In few words, a set of adequate combination of moments has been selected so that the related interaction matrix $\mathbf{L}_{\mathbf{s}}$ is as near as possible of a triangular matrix.

Finally, in 2D visual servoing, the behavior of the features in the image is generally satisfactory. On the other hand, the robot trajectory in 3D space is quite unpredictable and may be very unsatisfactory for large rotational displacements [2]. In fact, the difference of behaviors in image

space and 3D space is due to the non linearities that usually appears in the interaction matrix. In our method, the combinations of moment have been chosen to minimize the non linearities in \mathbf{L}_s (see [12] for more details).

2.2 Experimental results with binary planar objects of complex unknown shape

This section presents some experimental results obtained with a six dof eye-in-hand system. The moments are computed at video rate after a simple binarisation of the aquired image, without any spatial segmentation.

2.2.1 Complex motion

We first test our scheme for a displacement involving very large translation and rotation to realize between the initial and desired images (see Figures 1.a and 1.b). The interaction matrix computed at the desired position has the following form:

$$\mathbf{L}_s|_{s=s^*} = \begin{pmatrix} -1 & 0 & 0 & 0.01 & -0.52 & 0.01 \\ 0 & -1 & 0 & 0.51 & -0.01 & 0.01 \\ 0 & 0 & -1 & -0.02 & -0.01 & 0 \\ 0 & 0 & 0 & -0.33 & -0.62 & 0 \\ 0 & 0 & 0 & -0.61 & 0.09 & 0 \\ 0 & 0 & 0 & -0.04 & -0.08 & -1 \end{pmatrix} \quad (2)$$

We can note that this matrix is block triangular with main terms around the diagonal. The value of its condition number (equal to 2.60) is also very satisfactory. The obtained results are given on Figure 1. They show the good behavior of the control law. First, we can note the fast convergence towards the desired position. Then, there is no oscillation in the decrease of the visual features (see Figure 1.c), and there is only one small oscillation for only two components of the camera velocity (see Figure 1.d). Finally, even if the rotation to realize between the initial and the desired positions is very large, the obtained camera 3D trajectory is satisfactory (see Figure 1.e), while it was an important drawback for classical 2D visual servoing.

2.2.2 Results with a bad camera calibration and object occlusion

We now test the robustness of the method with respect to a bad calibration of the system. In this experiment, errors have been added to camera intrinsic parameters (25% on the focal length and 20 pixels on the coordinates of the principal point) and to the object plane parameters ($\hat{Z}^* = 0.8m$ instead of $Z^* = 0.5m$ where Z^* is the desired depth between the camera and the object). We can also notice that the lighting conditions for the desired and the initial positions given on Figure 2.a and 2.b are different. Furthermore, an occlusion has been generated since the object is

not completely in the camera field of view at the beginning of the servo. The obtained results are given in Figure 2. We can notice that the system converges despite the worse conditions of experimentations and, as soon as the occlusion ends (after iteration 30), the behavior of the system is similar to those of the previous experiment, which validates the robustness of our scheme with respect to modeling errors.

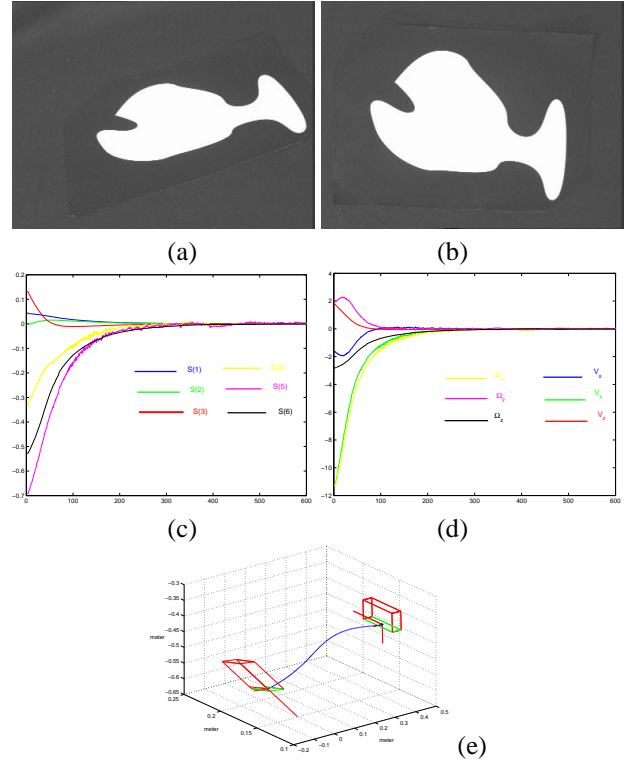


Figure 1: Results for a complex motion: (a) initial image, (b) desired image, (c) visual features ($s - s^*$), (d) camera velocity \mathbf{T}_c , (e) camera 3D trajectory

2.3 Experimental results with objects composed of a set of points

In this paragraph, we present similar experimental results obtained with objects composed of a set of points (see Figure 3). The considered points have been extracted using Harris detector and tracked using a SSD algorithm. We can note however that the plots are noisy. It is mainly noticeable on the ω_x and ω_y components of the camera velocity whose value depends on 5th order moments (while ω_z and v_z are not noisy at all since their value only depend of moments of order 2). Despite this noise, the exponential decrease, the convergence and stability are still obtained, which proves the validity of our approach. This results can

even be improved using a sub pixel accuracy image tracker such as Shi-Tomasi algorithm [13].

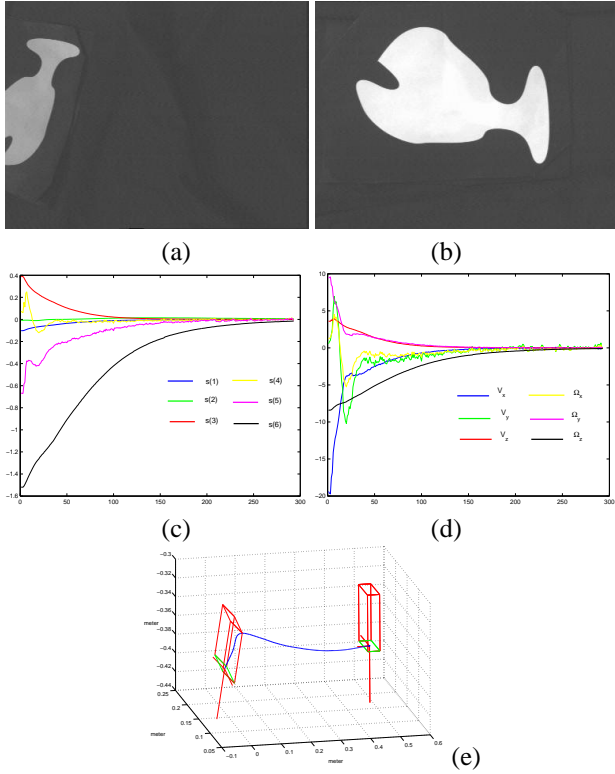


Figure 2: Results using a bad camera calibration: (a) initial image, (b) desired image, (c) visual features ($s - s^*$), (d) camera velocity, (e) camera 3D trajectory

3 Robust model-based tracking

3.1 Overview of the approach

This section addresses the problem of realizing visual servoing tasks by using complex objects in real environments. For that, we present a real-time model-based tracking of objects in monocular image sequences. This fundamental vision problem has applications in many domains ranging from augmented reality to visual servoing and even medical imaging or industrial applications. The main advantage of a model-based method is that the knowledge about the scene (the implicit 3D information) allows improvements of robustness and performance by being able to predict hidden movement of the object and acts to reduce the effects of outlier data introduced in the tracking process.

In the related literature, geometric primitives considered for the estimation are often points[4], segments, lines, contours or points on the contours, conics, cylindrical objects or a combination of these different features. Another im-

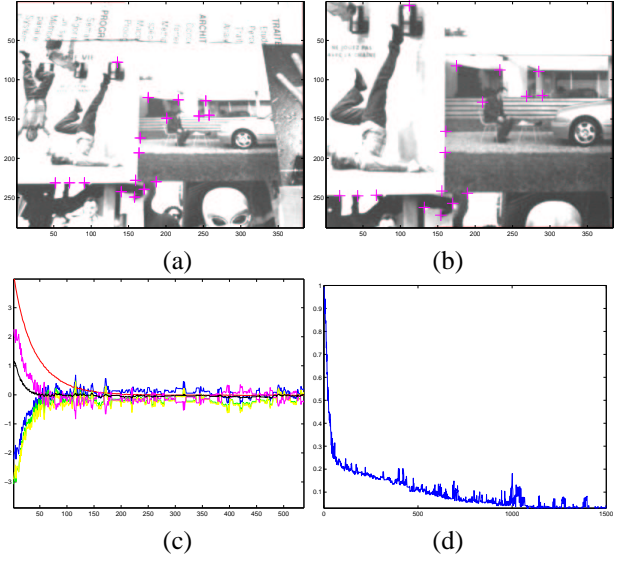


Figure 3: Results for complex images: (a) initial image, (b) desired image, (c) velocities, (d) features errors mean

portant issue is the registration problem. *Purely geometric*, or *numerical and iterative* approaches may be considered. *Linear approaches* use a least-squares method to estimate the pose. *Full-scale non-linear optimization techniques* (e.g., [9, 5, 8]) consists of minimizing the error between the observation and the forward-projection of the model. In this case, minimization is handled using numerical iterative algorithms such as Newton-Raphson or Levenberg-Marquardt. The main advantage of these approaches are their accuracy. The main drawback is that they may be subject to local minima and, worse, divergence.

Our method is fully described in [3]. Pose computation is formulated in terms of a full scale non-linear optimization using a 2D virtual visual servoing scheme [11, 14]. Our method takes the 2D visual servoing framework by controlling the motion of a virtual camera so that the projection in the image of the object model perfectly fits with the current position of the object in the image acquired by the real camera. We thus obtain an image feature-based system which is capable of treating complex scenes in real-time without the need for markers. Contributions can be exhibited at three different levels:

- the analytical form of the interaction matrices L_s related to complex visual features including ellipses, cylinders, points, distances and any combination of these is easily obtained [6]. Determining an accurate approximation of this matrix is essential to obtain the convergence of the visual servoing. In [3], a complete derivation of interaction matrices for distances to lines, ellipses and cylinders are given. Furthermore, computational efficiency is obtained by 'stacking' in-

teraction matrices and by using a constant interaction matrix \widehat{L}_s in the control law.

- the widely accepted statistical techniques of robust M-estimation are employed. This is introduced directly in the virtual visual servoing control law by weighting the confidence on each feature. The Median Absolute Deviation (MAD) is used as an estimate of the standard deviation of the inlier data. Statistically robust pose computation algorithm, suitable for real-time tracking techniques, have been considered.
- the formulation for tracking objects is dependent on correspondences between local features in the image and the object model. In an image stream, these correspondences are given by the local tracking of features in the image. In our method, low level tracking of the contours is implemented via an adequate algorithm, called Moving Edges algorithm [1]. A local approach such as this is ideally suited to real-time tracking due to an efficient 1D search normal to a contour in the image. In a 'real world' scenario, some features may be incorrectly tracked, due to occlusion, changes in illumination and miss-tracking. Since many point-to-curve correspondences are made, the method given here has many redundant features which favors the use of robust statistics.

3.2 Tracking results in visual servoing experiments

Any visual servoing control law can be used using the output of our tracker (image-based, position-based or hybrid scheme). In the presented experiments, we have considered a now well known 2 1/2D approach, already described in [10]. It consists in combining visual features obtained directly from the image, and features expressed in the Euclidean space. The 3D information can be retrieved either by a projective reconstruction obtained from the current and desired images, either by a pose estimation algorithm. In our context, since the pose is an output of our tracker, we consider in this paper the latter solution.

The complete implementation of the robust visual servoing task, including tracking and control, was carried out on an experimental test-bed involving a CCD camera mounted on the end effector of a six d.o.f robot. Images were acquired and processed at video rate (50Hz).

In such experiments, the image processing is potentially very complex. Indeed extracting and tracking reliable points in real environment is a non trivial issue. The use of more complex features such as the distance to the projection of 3D circles, lines, and cylinders has been demonstrated in [3] in an augmented reality context. In all experiments, the distances are computed using the Moving

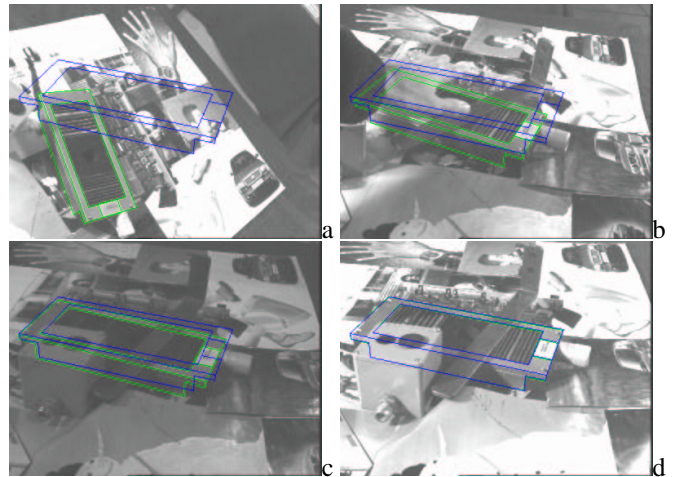


Figure 4: Tracking in complex environment within a classical visual servoing: Images are acquired and processed at video rate (25Hz). Blue: desired position defined by the user. Green: position measured after pose calculation. (a) first image initialized by hand, (b) partial occlusion with hand, (c) lighting variation, (d) final image with various occlusions

Edges algorithm previously described. Tracking is always performed at below frame rate (usually in less than 10ms).

In all the figures depicted, current position of the tracked object appears in green while its desired position appears in blue. Three objects were considered: a micro-controller (Figure 4), an industrial emergency switch (Figure 5) and a video multiplexer (Figure 6).

To validate the robustness of the algorithm, the objects were placed in a highly textured environment as shown in Fig. 4, 5 and 6. Tracking and positioning tasks were correctly achieved. Multiple temporary and partial occlusions by an hand and various work-tools, as well as modification of the lighting conditions were imposed during the realization of the positioning task. On the third experiments (see Figure 6), after a complex positioning task (note that some object faces appeared while other disappeared) the object is handled by hand and moved around. Since the visual servoing task has not been stopped, robot is still moving in order to maintain the rigid link between the camera and the object.

For the second experiment, plots are also shown which help to analyse the pose parameters estimation, the camera velocity and the error vector. In the second experiment, the robot velocity reaches 23 cm/s in translation and 85 dg/s in rotation. In other words, less than 35 frames were acquired during the entire positioning task up until convergence (see Figure 5e). Therefore the task was accomplished in less than 1 second. In all these experiments, neither a Kalman filter (or other prediction process) nor the camera displace-

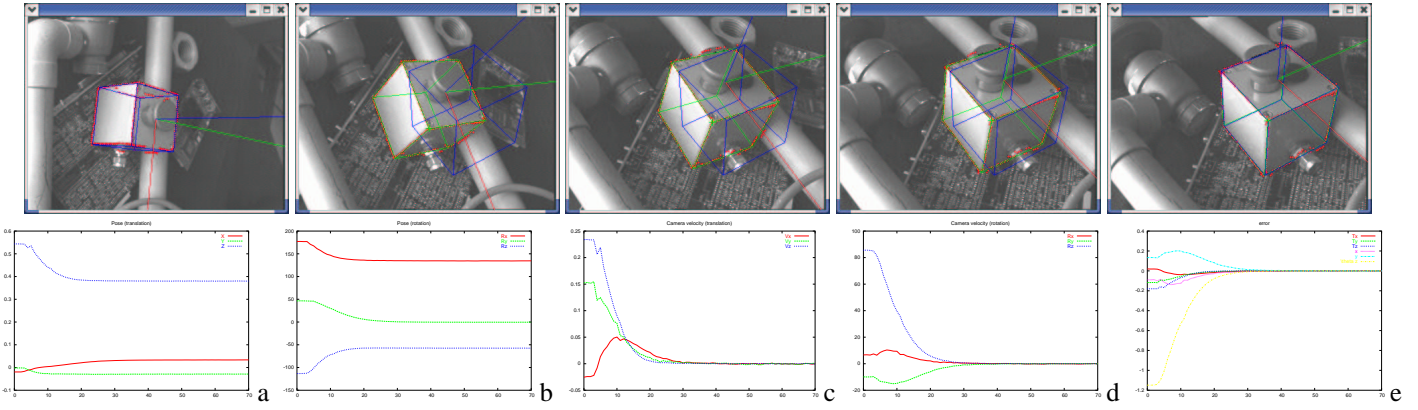


Figure 5: 2D 1/2 visual servoing experiments: on these five snapshots, the tracked object appears in green and its desired position in the image in blue. Plots correspond to (a) pose (translation), (b) pose (rotation), (c-d) camera velocity in rotation and translation, (e) error vector $s - s^*$

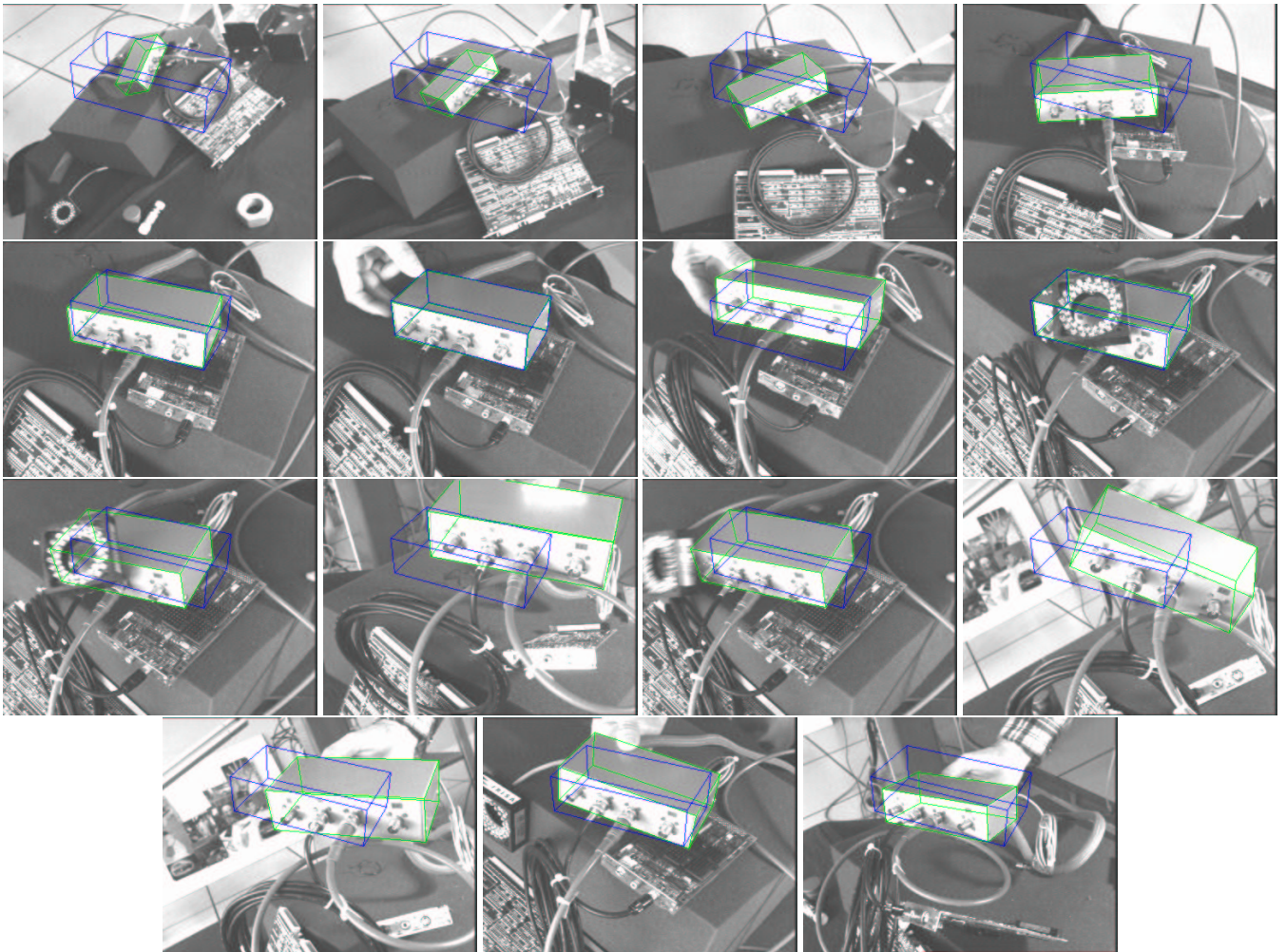


Figure 6: 2D 1/2 visual servoing experiments: on these snapshots the tracked object appears in green and its desired position in the image in blue. The six first images have been acquired during an initial visual servoing step where the object is motionless. In the reminder images, object is moving along with the robot.

ment were used to help the tracking.

References

- [1] P. Bouthemy. A maximum likelihood framework for determining moving edges. *IEEE Trans. on Pattern Analysis and Machine intelligence*, 11(5):499–511, May 1989.
- [2] F. Chaumette. Potential problems of stability and convergence in image-based and position-based visual servoing, *The Confluence of Vision and Control*, pp. 66–78, *LNCIS Series*, No 237, Springer-Verlag, 1998.
- [3] A. Comport, E. Marchand, and F. Chaumette. A real-time tracker for markerless augmented reality. *ACM/IEEE Int. Symp. on Mixed and Augmented Reality, ISMAR'03*, pp. 36–45, Tokyo, Japan, October 2003.
- [4] D. Dementhon and L. Davis. Model-based object pose in 25 lines of codes. *Int. J. of Computer Vision*, 15:123–141, 1995.
- [5] T. Drummond and R. Cipolla. Real-time visual tracking of complex structures. *IEEE Trans. on Pattern Analysis and Machine Intelligence*, 27(7):932–946, July 2002.
- [6] B. Espiau, F. Chaumette, P. Rives: A new approach to visual servoing in robotics, *IEEE Trans. on Robotics and Automation*, 8(3):313–326, June 1992.
- [7] S. Hutchinson, G. Hager, P. Corke: A tutorial on visual servo control, *IEEE Trans. on Robotics and Automation*, 12(5):651–670, October 1996.
- [8] D. Kragic and H.I. Christensen. Confluence of parameters in model based tracking. In *IEEE Int. Conf. on Robotics and Automation, ICRA'03*, volume 4, pages 3485–3490, Taipei, Taiwan, September 2003.
- [9] D. Lowe. Robust model-based motion tracking through the integration of search and estimation. *Int. Journal of Computer Vision*, 8(2):113–122, 1992.
- [10] E. Malis, F. Chaumette, and S. Boudet. 2 1/2 D visual servoing. *IEEE Trans. on Robotics and Automation*, 15(2):238–250, April 1999.
- [11] E. Marchand and F. Chaumette. Virtual visual servoing: a framework for real-time augmented reality. *Eurographics'02 Conf. Proc.*, Vol. 21(3) of *Computer Graphics Forum*, pp. 289–298, Saarebrücken, Germany, September 2002.
- [12] O. Tahri, F. Chaumette. Application of moment invariants to visual servoing *IEEE Int. Conf. on robotics and Automation, ICRA'03*, Vol. 3, pp. 4276–4281, Taipei, Taiwan, September 2003.
- [13] J. Shi and C. Tomasi. Good features to track. In *IEEE Int. Conf. Computer Vision and Pattern Recognition, CVPR'94*, pages 593–600, Seattle, June 1994.
- [14] V. Sundareswaran and R. Behringer. Visual servoing-based augmented reality. In *IEEE Int. Workshop on Augmented Reality*, San Francisco, November 1998.